THE JOURNAL OF BIOLOGICAL CHEMISTRY
Vol. 279, No. 32, Issue of August 6, pp. 33716–33726, 2004

Printed in U.S.A.

Polyisoprenylated Benzophenone, Garcinol, a Natural Histone Acetyltransferase Inhibitor, Represses Chromatin Transcription and Alters Global Gene Expression*

Received for publication, March 12, 2004, and in revised form, May 12, 2004
Published, JBC Papers in Press, May 19, 2004, DOI 10.1074/jbc.M402839200

Karanam Balasubramanyam‡§¶, M. Altaf‡§, Radhika A. Varier‡, V. Swaminathan‡, Aarti Ravindran‖, Parag P. Sadhale‖, and Tapas K. Kundu‡ ‡‡**

From the ‡Transcription and Disease Laboratory, Molecular Biology and Genetics Unit, Jawaharlal Nehru Centre for Advanced Scientific Research, Jakkur, Bangalore-560064 and the ‖Department of Microbiology and Cell Biology, Indian Institute of Science Bangalore-560012, India

Histone acetylation is a diagnostic feature of transcriptionally active genes. The proper recruitment and function of histone acetyltransferases (HATs) and deacetylases (HDACs) are key regulatory steps for gene expression and cell cycle. Functional defects of either of these enzymes may lead to several diseases, including cancer. HATs and HDACs thus are potential therapeutic targets. Here we report that garcinol, a polyisoprenylated benzophenone derivative from *Garcinia indica* fruit rind, is a potent inhibitor of histone acetyltransferases p300 (IC_{50} ≈7 μM) and PCAF (IC_{50} ≈5 μM) both *in vitro* and *in vivo*. The kinetic analysis shows that it is a mixed type of inhibitor with an increased affinity for PCAF compared with p300. HAT activity-dependent chromatin transcription was strongly inhibited by garcinol, whereas transcription from DNA template was not affected. Furthermore, it was found to be a potent inducer of apoptosis, and it alters (predominantly down-regulates) the global gene expression in HeLa cells.

The acetylation and deacetylation of histones play a key role in the regulation of gene expression in eukaryotic cells (1). The acetylation status of histones alters chromatin structure and thereby modulates gene expression. Two classes of enzymes can effect the acetylation of histones, histone acetyltransferases (HATs),[1] and histone deacetylases (HDACs) (1, 2). Interestingly, these enzymes can also acetylate or deacetylate several non-histone substrates with functional consequences (1, 3). Altered HAT and HDAC activities can lead to several diseases, ranging from cancer to neurodegenerative diseases (4–7).

Several families of HATs have recently been identified, which includes the GNAT family (GCN5-related *N*-acetyltransferase), the MYST group, SAS2, TIP60, and p300/CBP families (1, 3). The p300/CBP family of HAT is represented by two of the most widely studied HATs, p300 and CBP. These proteins share considerable sequence and functional homology. Several lines of evidence indicate that p300/CBP are involved in cell cycle progression and cellular differentiation (8–11). Mechanistically, these proteins function as transcriptional coactivators through their direct interaction with a diverse group of transcription factors and the RNA polymerase II transcription machinery. The coactivation function is partially facilitated by their intrinsic HAT activity (12, 13). Mutations in the HAT active site abolish transactivating function (1). The p300/CBP-associated factor, PCAF is one of the important HATs of the GNAT family. The C-terminal-half of PCAF has a highly significant sequence similarity to yeast GCN5 (14). In humans there are two GCN5 splice variants, hGCN5 and hGCN5-L (long form) synthesized from the same gene. The hGCN5-L is similar in length to PCAF and shares 75% amino acid sequence identity with PCAF. It also interacts with p300/CBP. The hGCN5-L is thus termed as PCAF-B (15). *PCAF-B* is an essential gene expressed ubiquitously early in development, whereas PCAF is expressed later in embryonic development and is not essential (16). *In vivo* PCAF exists in a large multiprotein complex, containing more than 20 different polypeptides (17). Unlike p300/CBP (which acetylates all the four core histones, predominantly H3 and H4) PCAF acetylates predominantly histone H3. For nucleosomal histone substrates, this specificity is quite exclusive. The acetylase domain of PCAF is required for MyoD-dependent coactivation and differentiation. Presumably the acetyltransferase activity of PCAF and PCAF-B is also involved in DNA repair (15). Both p300/CBP and PCAF also target non-histone protein substrates, which include, human transcriptional coactivators, PC4 (18), HMGB-1 (19), HMG17, HMGI/Y; transcription factors E2F, p53, GATA1 (3), and HIV Tat protein (20, 21). The acetylation of these factors alters their DNA/nucleosome binding and/or protein-protein interactions and consequently influences their effect in regulating gene transcription.

It is thus evident that proper balance of acetylation and deacetylation is important for normal cell proliferation, growth, and differentiation. The dysfunction of these machineries leads to different diseases. Several lines of evidence indicate that HAT activity is associated with tumor suppression, and the loss or misregulation of this activity may lead to cancer. For exam-

* This work was supported by Jawaharlal Nehru Center for Advanced Scientific Research, Department of Science and Technology (DST), Government of India and Dabur Research Foundation (DRF). The costs of publication of this article were defrayed in part by the payment of page charges. This article must therefore be hereby marked "*advertisement*" in accordance with 18 U.S.C. Section 1734 solely to indicate this fact.

§ These authors contributed equally to this work.
¶ Present address: Dept. of Pharmacology, Johns Hopkins School of Medicine, 725 N. Wolfe St., Baltimore, MD 21205.

** Recipient of DST, DBT, CSIR, and ICMR Government of India grants.

‡‡ To whom correspondence should be addressed: Transcription and Disease Laboratory, Molecular Biology and Genetics Unit, Jawaharlal Nehru Centre for Advanced Scientific Research, Jakkur, Bangalore-560064, India. Tel.: 0091-80-23622750 (ext. 2257); Fax: 0091-80-23622766; E-mail: tapas@jncasr.ac.in.

[1] The abbreviations used are: HAT, histone acetyltransferase; PCAF, p300/CBP-associated factor; HDAC, histone deacetylase; TSA, trichostatin A; CTPB, *N*-(4-chloro-3-trifluoromethyl-phenyl)-2-ethoxy-6-pentadecyl-benzimidine; PBS, phosphate-buffered saline; Me_2SO, dimethyl sulfoxide.

ple, viral oncogene proteins E1A target p300/CBP, disrupting its interaction with PCAF (14). E1A interaction with p300/CBP is essential for cellular transformation. Chromosomal translocations associated with certain leukemias indicate that gain-of-function mutations in CBP is also oncogenic (22). Mutations in HATs cause several other disorders other than cancer. Mutations in CBP result(s) in the Rubinstein-Taybi syndrome (RTS) (23). It was found that a single mutation at the PHD domain of CBP causes this syndrome. Interestingly, this mutation (G to C at 4951) in CBP also abolishes its HAT activity (23, 24). Degradation of CBP/p300 was found to be associated with certain neurodegenerative diseases (7). Proper HAT function is also essential for the replication of HIV. It was elegantly shown that treatment with HDAC inhibitors inhibits the latency of HIV, presumably by inducing acetylation of Tat protein and the nucleosomes on the LTR (25, 26). These examples clearly indicate that histone acetyltransferases and deacetylases should be one of the potential targets for therapy. During the last decade, a number of HDAC inhibitors have been identified that induce apoptosis in cultured tumor cells (4). These inhibitors were also found to be potent anticancer agents *in vivo*. Furthermore, some of these inhibitors (*e.g.* SAHA) are already in human trial as antineoplastic drug (27). Although substantial progress has been made in the study of HDAC inhibitors, very little is known about HAT inhibitors. Initially, before the discovery of HATs, polyamine-CoA conjugates were found to inhibit the acetyltransferase activity of cell extracts (28). Availability of recombinant HATs (p300 and PCAF) made it possible to synthesize more targeted specific inhibitors, Lys-CoA for p300 and H3-CoA-20 for PCAF (29). However, these inhibitors could not permeate the cells and were found to be pharmacogenically poor (30). Recently, we have discovered a natural inhibitor anacardic acid from cashew nut shell liquid that potently inhibits both p300 and PCAF (31). Based on anacardic acid we have synthesized a small molecule activator of p300, CTPB. Interestingly, CTPB is specific for p300. Both anacardic acid and CTPB may serve as potential lead compounds for designing different drugs.

Here we report that a polyisoprenylated benzophenone, garcinol, isolated from *Garcinia indica* (an edible fruit) is a potent inhibitor of histone acetyltransferases p300 and PCAF. It also inhibits histone acetylation *in vivo* but has no effect on deacetylation of histones. Interestingly, though garcinol repressed the p300 HAT-dependent chromatin transcription, it had no effect on naked DNA transcription. Furthermore microarray analysis of gene expression in garcinol-treated HeLa cells showed that it represses transcription globally with an appreciable chromosome bias.

EXPERIMENTAL PROCEDURES

Purification of Human Core Histones and Recombinant Proteins—Human core histones were purified from HeLa nuclear pellet as described previously (32). The FLAG epitope-tagged human histone deacetylase 1 (HDAC1), and PCAF were purified from the recombinant baculovirus-infected insect cell line Sf21 by immunoaffinity purification using M2 agarose (Sigma) (32). Full-length p300 was also purified from the recombinant baculovirus-infected Sf21 cells as a His_6-tagged protein through the nickel-nitrilotriacetic acid affinity column (Qiagen) as described previously (12). The His_6-tagged nucleosome assembly protein 1 (NAP1) used for the *in vitro* chromatin assembly was purified from *Escherichia coli* cells as reported previously (32). The FLAG-tagged chimeric activator Gal4-VP16 was expressed in *E. coli* and purified by immunoaffinity purification with M2 agarose (Sigma) (12). His_6-tagged D-topoisomerase 1 (catalytic domain) was expressed in *E. coli* and purified as described earlier (33).

Purification and Structural Analysis of Garcinol—Garcinol was prepared from *Garcinia indica* fruit rind (46). In brief, *G. indica* dried fruit (Kokum) rind was extracted with ethanol, and the extract was fractionated by ODS (octadecyl silica) column chromatography eluted stepwise with 60–80% aqueous ethanol. The fractions containing garcinol were concentrated and dried in vacuum. The residue was dissolved in hexane, and the solution was cooled at 5 °C for 2 days. Yellow amorphous precipitate was collected from the solution and washed with cold hexane and recrystallized at room temperature. Pale yellow needle crystals were obtained from the solvent, which were identified as garcinol from the following spectral data: mp 126 °C; Optical rotation at 30–135 ($CHCl_3$); UV in EtOH (log ϵ) 367 (3.84) and 250 (4.05) nm; IR 3200–3500, 1730, 1640 cm^{-1}; ^1H NMR ($CDCl_3$) δ 6.95 (1H, dd, J = 9.0 and 2.0 Hz), 6.91 (1H, d, J = 2.0 Hz), 6.60 (1H, d, J = 9.0 Hz), 4.96, 5.06, 5.10 (1H each, t, J = 5.0 Hz), 4.40 (d, J = 15.0 Hz), 2.80–1.46 (m, 12H, methylene and methyne), 1.78, 1.74, 1.69, 1.62, 1.59, 1.56, 1.21, 1.05 (3H each, s); EI-MS *m/z* 602 $[M]^+$, 533, 465, 341.

HAT Assay—The protocol used for the HAT assays is described elsewhere (32). Indicated amounts of proteins (see figure legends) were incubated in HAT assay buffer containing 50 mM Tris-HCl, pH 8.0, 10% (v/v) glycerol, 1 mM dithiothreitol, 1 mM phenylmethylsulfonyl fluoride, 0.1 mM EDTA pH 8.0, 10 mM sodium butyrate at 30 °C for 10 min in the presence and absence of garcinol followed by addition of 1 μl of 4.7 Ci/mmol [^{3}H]acetyl-CoA and were further incubated for another 10 min. The final reaction volume was 30 μl. The reaction mixture was then blotted onto P-81 (Whatman) filter paper and radioactive counts were recorded on a Wallace 1409 liquid scintillation counter. To visualize radiolabeled acetylated histones, the reaction products were resolved on 15% SDS-polyacrylamide gel and subjected to fluorography followed by autoradiography as described earlier (32). For the kinetic analysis of garcinol-mediated inhibition of HATs, a filter binding assay was performed as described in figure legends (Fig. 3).

HDAC Assay—The deacetylation assay was performed as described previously (31), Briefly 2.4 μg of core histones were incubated in HAT buffer without NaBu, with 20 ng of p300 and 1 μl of 4.7 Ci/mmol [^{3}H]acetyl-CoA for 30 min at 30 °C. The activity of p300 was inhibited by incubating the reaction mixture with 10 nM p300-specific inhibitor lysyl-CoA (29) for 15 min at 30 °C, after which 50 ng of HDAC1 was added in the presence or absence of garcinol and incubated further for 45 min at 30 °C. The samples were analyzed as described above.

Analysis of in Vivo Acetylated Histones by Acid/Urea/Triton (AUT) Polyacrylamide Gel Electrophoresis—HeLa cells (3×10^6 cells per 90-mm dish) were seeded overnight, and histones were extracted from the cells after 24 h of compound treatment as described elsewhere (34). Briefly, cells were harvested, washed in ice-cold buffer A (150 mM KCl, 20 mM HEPES, pH 7.9, 0.1 mM EDTA, and 2.5 mM $MgCl_2$) and lysed in buffer A containing 250 mM sucrose and 1% (v/v) Triton X-100. Nuclei were recovered by centrifugation, washed, and proteins were extracted for 1 h using 0.25 M HCl. Chromosomal proteins were precipitated with 25% (w/v) trichloroacetic acid and sequentially washed with ice-cold acidified acetone (20 μl of 12 N HCl in 100 ml of acetone), and acetone, air-dried, and dissolved in the sample buffer (5.8 M urea, 0.9 M glacial acetic acid, 16% glycerol, and 4.8% 2-mercaptoethanol). The protein was quantified using a protein assay reagent (Bio-Rad). The histones were resolved on AUT gel as described elsewhere (35, 36). Briefly, 8 cm of the separating gel (1 M acetic acid, 8 M urea, 0.5% Triton X-100, 45 mM NH_3, 18% acrylamide mix, and 0.5% TEMED) was overlaid with 2 cm of an upper gel (1 M acetic acid, 8 M urea, 0.5% Triton X-100, 45 mM NH_3, 3.3% acrylamide, 0.16% bisacrylamide, and 0.5% TEMED) and polymerization was aided with 0.0003% riboflavin. The gel was pre-electrophoresed for 3–4 h at 130 V in running buffer (1 M acetic acid) until the current no longer dropped. Fresh running buffer was added prior to loading the samples (0.2% methyl green was added as the tracking dye), and the gel was run overnight at 130 V and subsequently stained with Coomassie Brilliant Blue.

In Vitro Chromatin Assembly—Chromatin template for *in vitro* transcription experiments was assembled and characterized as described earlier (12).

In Vitro Transcription Assay—Transcription assays were essentially carried out as described previously (12) with some modifications. The scheme of transcription has been depicted in Fig. 5*A*. Briefly, the reconstituted chromatin template (containing 30 ng of DNA) or an equimolar amount of histone-free DNA was incubated with 50 ng of activator (Gal4-VP16) in a buffer containing 4 mM HEPES (pH 7.8), 20 mM KCl, 2 mM dithiothreitol, 0.2 mM phenylmethylsulfonyl fluoride, 10 mM sodium butyrate, 0.1 mg/ml bovine serum albumin, 2% glycerol. p300 was preincubated with indicated amounts of garcinol at 20 °C for 20 min following which it was added to the transcription reaction and incubated for 30 min at 30 °C. After acetylation, HeLa nuclear extract (5 μl, which contains 8 mg/ml protein) was added to initiate the preinitiation complex formation. Transcription reaction was started by the addition of NTP mix and α-[^{32}P]UTP after the preinitiation complex formation. The incubation was continued for 40 min at 30 °C. A sepa-

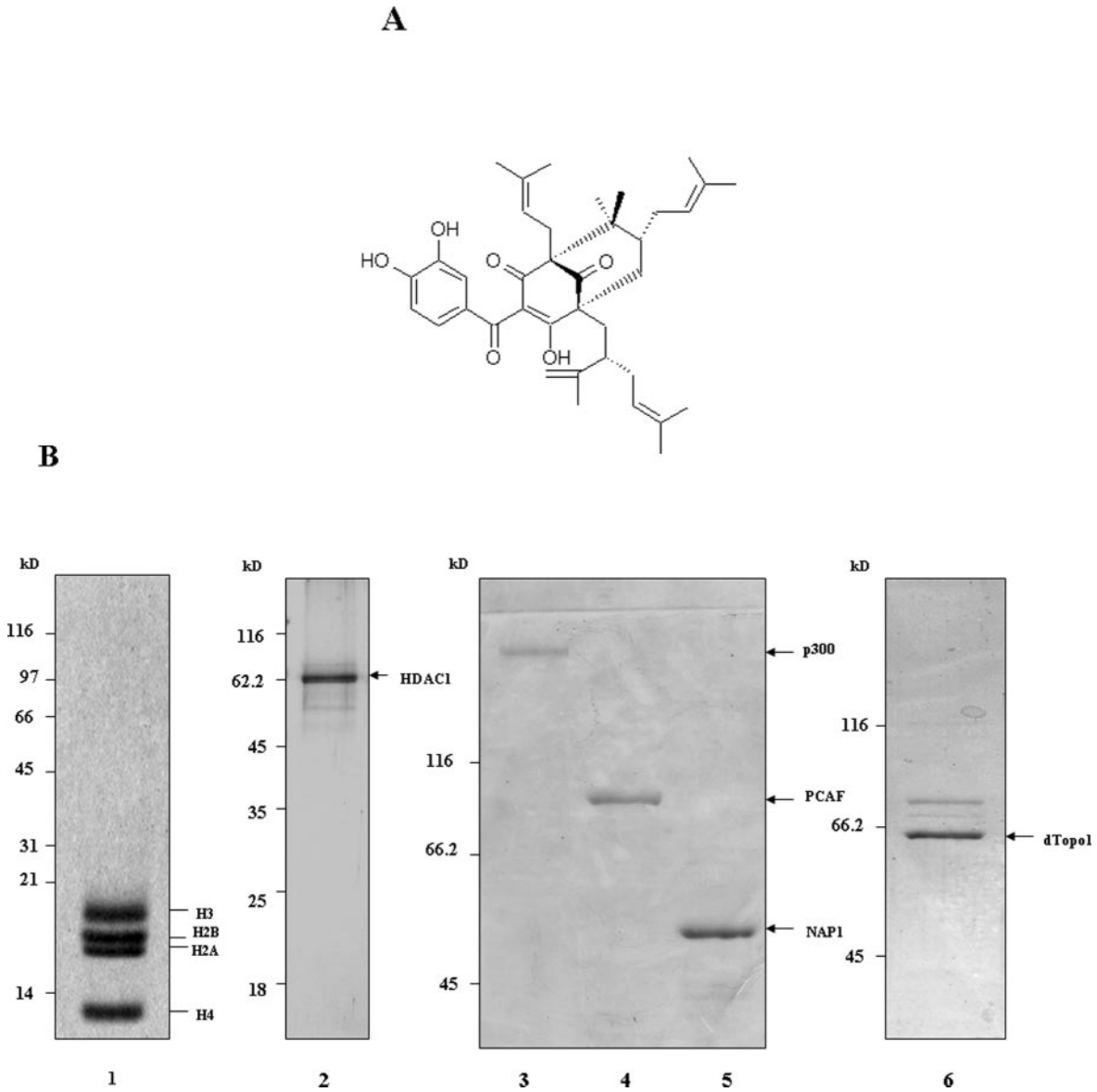

FIG. 1. *A*, chemical structure of garcinol. *B*, purified proteins used in different experiments. Highly purified core histones (3 μg) from HeLa nuclear pellet were analyzed on 15% SDS-PAGE. *Lane 1*, visualized by Coomassie Blue staining; *lane 2*, 300 ng of baculovirus-expressed FLAG epitope-tagged, full-length human HDAC1 analyzed on 10% SDS-PAGE; *lane 3*, 150 ng of full-length, His_6-tagged p300; *lane 4*, 200 ng of FLAG epitope-tagged full-length PCAF; *lane 5*, 300 ng of His_6-tagged mouse NAP1 each analyzed on 8% SDS-PAGE; *lane 6*, 300 ng of *E. coli* expressed His_6-tagged *Drosophila* toposiomerase 1 (catalytic domain) were analyzed on 8% SDS-PAGE stained with Coomassie Blue.

rate reaction was setup with ~25 ng of supercoiled ML200 DNA, and the transcription assay was carried out as described above, without the addition of the activator (Gal4-VP16). 2 μl of this reaction was added to each of the transcription reactions to serve as a loading control. The transcription reactions were terminated by the addition of 250 μl of stop buffer (20 mM Tris-HCl, pH 8.0, 1 mM EDTA, 100 mM NaCl, 1% SDS, and 0.025 ng/μl tRNA). Transcripts were analyzed by 5% Urea-PAGE and visualized by autoradiography. Quantification of transcription was done by phosphorimager (Fuji) analysis.

Apoptosis Assay—Garcinol-induced apoptosis was monitored by the extent of chromatin fragmentation. DNA was extracted from the untreated and garcinol-treated HeLa cells. The cells (3×10^6 per 90-mm dish) were seeded and treated with the compound for 24 h. Harvested cells were washed with PBS and then lysed with lysis buffer containing 0.5% Triton X-100, 20 mM Tris, and 15 mM EDTA at room temperature for 15 min. The lysate was treated with RNase (0.1 mg/ml) and proteinase K (2 mg/ml) for 1 h, extracted with phenol/chloroform/isoamyl alcohol (25:24:1), and DNA was precipitated by incubating the upper aqueous phase with 0.1 volumes of 3 M sodium acetate (pH 5.2) and 1 volume of isopropyl alcohol overnight at −20 °C. The pellet obtained on centrifugation was washed with 70% ethanol and dissolved after air-drying in 50 μl of TE buffer. The extracted DNA was analyzed on a 1.8% agarose gel and visualized by ethidium bromide staining. Nuclei fragmentation was also visualized by Hoechst staining of apoptotic nuclei. The apoptotic cells were collected by centrifugation, washed with PBS and fixed in 4% paraformaldehyde for 20 min at room temperature. Subsequently the cells were washed and resuspended in 20 μl of PBS before depositing it on polylysine-coated coverslips. The cells were left to adhere on cover slips for 30 min at room temperature after which the cover slips were washed twice with PBS. The adhered cells were then incubated with 0.1% Triton X-100 for 5 min at room temperature and rinsed with PBS for three times. The coverslips were treated with Hoechst 33258 for 30 min at 37 °C, rinsed with PBS, and mounted on slides with glycerol-PBS. Stained nuclei were analyzed by using Axioskop-2- plus upright microscope with epi-fluorescence equipment (Carl Zeiss), and the image was captured by Axiocam MRC camera and analyzed by AxioVision 3.1 software.

Microarray Analysis—The microarrays used in this study were procured from the Microarray center, University Health Network, Toronto, Ontario. Each array carries 19,200 spots from the human genome, arranged in 48 individual arrays of 400 spots each. Each of the 48 grids contains 3 *Arabidopsis* spots that serve as local controls. The total RNA was isolated from control and treated cells using RNaeasy kit (Sigma, 74103). The micromax indirect labeling kit (PerkinElmer Life Sciences, MPS521) was used to synthesize the labeled cDNA from 4 μg of total RNA and further process the hybridized cDNA on the array by the

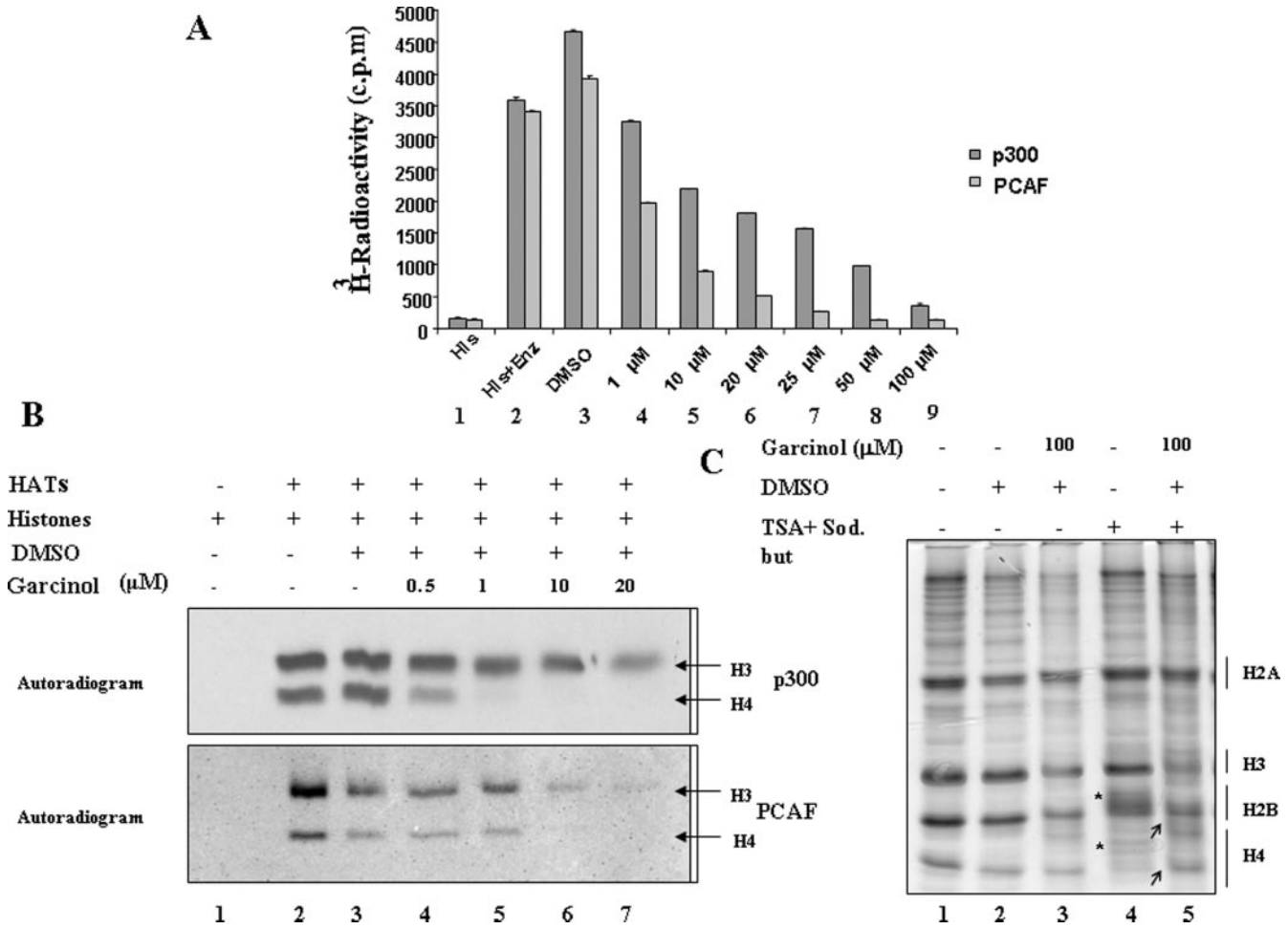

FIG. 2. **Garcinol is a potent inhibitor of HATs.** HAT assays were performed either with p300 or PCAF in the presence or absence of garcinol using highly purified HeLa core histones (800 ng) and processed for filter binding (*A*) or fluorography (*B*). For fluorography, reaction mixtures were analyzed on 15% SDS-polyacrylamide gel and exposed to x-ray film for 72 h. *Lane 1,* core histones without any HAT; *lane 2,* histones with HAT; *lane 3*, histones with HAT and in the presence of Me_2SO as solvent control; *lanes 4–7*, histones with HAT and in the presence of 0.5, 1, 10, 20 μM concentrations of garcinol, respectively. *C*, effect of garcinol on cellular histone acetylation. HeLa cells were treated as indicated, for 24 h. Histones were acid-extracted and analyzed over 18% acid/urea/Triton-PAGE. The protein bands were visualized by Coomassie Brilliant Blue staining. Histones extracted from untreated cells (*lane 1*), Me_2SO- (*DMSO*, solvent control) treated cells (*lane 2*), garcinol- (100 μM) treated cells (*lane 3*), trichostatin- (2 μM) and sodium butyrate- (10 mM) treated cells (*lane 4*), and trichostatin- A (2 μM), sodium butyrate- (10 mM), and garcinol- (100 μM) treated cells (*lane 5*) are shown. *Asterisk* (*) indicates hyperacetylation of histones H4 and H2B in response to HDAC inhibition by TSA and sodium butyrate. *Arrow* indicates inhibition of TSA-induced hyperacetylation of H4 and H2B by garcinol.

tyramide signal amplification method (37). All steps were carried out according to manufacturer's recommendations (www.nen.com/pdf/penen264-mmaxaminated_card.pdf). The array slides were scanned immediately using a GenePix Presonal 4100A Axon Scanner. The images were analyzed using the GenePix software and the Genowizard software (Genotypic Technology, Bangalore) was used for grid wise normalization of the array. Six arrays were used with two biological repeats of the treatment of cells and at least two dye swap experiments were included in the final analysis. The genes that were picked up as differentially regulated had a log mean of at least 1.27489 with S.D. less than 20% of the expression change in the case of up-regulated genes and a log mean of almost −1.75726 with S.D. less than 37% of the expression change in case of the down-regulated genes. Guidelines set by MIAME were followed, and the raw microarray data will be deposited in the GEO data base (www.ncbi.nlm.nih.gov/geo/).

RESULTS AND DISCUSSION

Dysfunction of histone acetyltransferases may lead to several diseases, predominantly cancer. Plant extracts or compounds known to have anticancer or cancer chemopreventive activities could be a source of small molecule modulators of HATs. By employing a highly purified recombinant HAT assay system, we have initiated a systematic effort to discover these molecules. Interestingly, a polyisoprenylated benzophenone from *G. indica* fruit rind has been found to be a potent inhibitor of histone acetyltransferases. Structural analysis identified it as the antioxidant and cancer chemopreventive agent garcinol (Fig. 1*A*). The HAT inhibitory activity was assayed using baculovirus-expressed recombinant histone acetyltransferase p300 and PCAF (Fig. 1*B*, *lanes 3* and *4*) and highly purified HeLa core histones as substrate (Fig. 1*B*, *lane 1*). Garcinol was found to be a highly efficient inhibitor of PCAF acetyltransferase activity with an IC_{50} of ~5 μM. Under similar conditions the IC_{50} of the inhibitor for p300 acetyltransferase activity was ~7 μM (Fig. 2*A* and data not shown). These results suggest that although garcinol inhibits the HAT activity of both p300 and PCAF, it is relatively more potent as well as a faster inhibitor of PCAF compared with p300. In order to further confirm these results we analyzed HAT assay products on SDS-PAGE followed by fluorography. In agreement with the results of the p300 filter binding assay, it was found that the HAT activity of PCAF was almost completely inhibited by 10 μM garcinol compared with the Me_2SO control, (Fig. 2*B*, *lane 3 versus 6*) whereas even at 20 μM concentration, 5–10% of ^{3}H-labeled histone H3 could be detected (Fig. 2*B*, *lane 3 versus 7*). Interestingly it was found that acetylation of histone H4 by p300 was more sensitive to inhibition by garcinol compared with

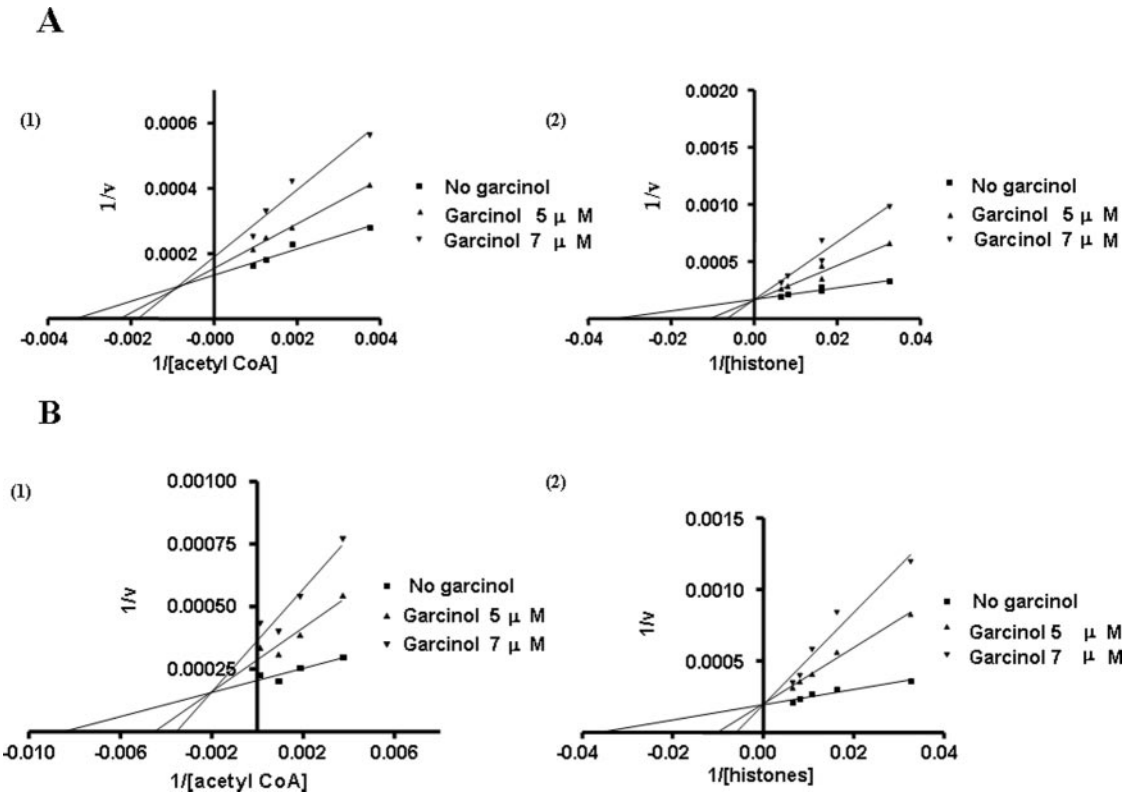

FIG. 3. **Inhibition kinetics of garcinol for p300 (*A*) and PCAF (*B*).** *A(1)*, and *B(1)*, Lineweaver-Burk plot showing the effect of garcinol on p300- and PCAF-mediated acetylation of highly purified HeLa core histones, respectively. HAT assays were carried out with a fixed concentration, of [^{3}H]acetyl-CoA (354 nM) and increasing concentrations of histones (0.033–0.165 μM) in the presence or absence of (5 and 7 μM) of garcinol. *A(2)*, and *B(2)*, depicting the same Lineweaver-Burk plot representation of garcinol effect on p300 and PCAF HAT activity at a fixed concentration of histone (8 pmol) and increasing concentrations of [^{3}H]acetyl-CoA in the presence (5 and 7 μM) or absence of garcinol. The results were plotted using GraphPad Prism software.

that of H3 (Fig. 2*B*, *top panel*, *lanes 4–7*). The p300-mediated acetylation of histone H4 was completely inhibited at a 1 μM concentration of garcinol, while 20 μM could not abolish the acetylation of H3 (Fig. 2*B*, *top panel*, *lane 5 versus lane 7*). After establishing garcinol as a strong inhibitor of HATs *in vitro*, we further investigated whether it could also affect the acetylation of histones *in vivo*. For this purpose HeLa cells were grown in monolayer (see "Experimental Procedures") and were treated with either Me_2SO (the solvent for garcinol) or different concentrations of garcinol. Histones were extracted from the cell pellet and analyzed on an 18% acid/urea/Triton polyacrylamide gel electrophoresis. As seen from the profile of different histones (Fig. 2*C*), incubation with the compound alone did not alter the acetylation status of the cellular histones significantly. In agreement with previous reports (38) the bulk histones from HeLa cells are found to be largely unacetylated (Fig. 2*C*, *lanes 1–3*). Because the global acetylation of histones for asynchronous cells does not change significantly, it was not possible to determine the effect of HAT inhibitor on histone acetylation. In order to stimulate histone acetylation, cells were treated with the deacetylase inhibitors TSA and sodium butyrate. As expected deacetylase inhibitors enhance the acetylation of histone H4 as well as H2B dramatically (Fig. 2*C*, *lane 4*). The treatment of the cells with garcinol along with TSA and sodium butyrate significantly inhibits the enhanced acetylation of H4 as well as H2B (Fig. 2*C*, compare *lane 4 versus 5* as indicated by an *arrow*). Taken together, these results establish that garcinol is a potent inhibitor of histone acetyltransferases *in vitro* and *in vivo*.

In order to understand the nature of inhibition as well as the mechanism of inhibition brought about by garcinol we analyzed the kinetics of inhibition for both p300 (Fig. 3*A*) and PCAF (Fig. 3*B*). The rate of the acetylation reaction at different concentrations of the inhibitor (and in its absence) was recorded with increasing concentrations of [^{3}H]acetyl-CoA and a constant amount of core histones as well as with increasing concentrations of core histones with constant amounts of [^{3}H]acetyl-CoA. The double reciprocal plot for each inhibitor concentration and in its absence was plotted as shown in Fig. 3. The kinetic results show that the inhibition patterns for p300 and PCAF are similar. When the concentration of acetyl-CoA was changed keeping the histone concentration constant, K_m increases, whereas V_{max} and k_{cat} of the reaction decrease (Fig. 3, *A* and *B*, *left panel* and Table I). On the other hand, increasing concentrations of histones with constant amounts of [^{3}H]acetyl-CoA increase K_m but V_{max} and k_{cat} remain the same (Fig. 3, *A* and *B*, *right panel* and Table I), which indicates that in this context garcinol competes with histones for binding to the active site of the enzyme and thus acts as a competitive inhibitor.

The reaction mechanism for p300 and PCAF to acetylate the lysine residues is contrastingly different. The GNAT family members, PCAF and serotonin *N*-acetyltransferase, and GCN5 employ ternary complex mechanisms that involve the ordered binding and release of substrates and products (39). On the other hand, the p300/CBP family follows the double displacement (ping-pong) mechanisms (40). The dead end analogue of acetyl-CoA, desulfo-CoA was shown to be a linear competitive inhibitor *versus* acetyl-CoA but it behaves as a linear uncompetitive inhibitor *versus* peptide substrate. Garcinol-mediated inhibition kinetics (for both p300 and PCAF) shows that with changing concentrations of acetyl-CoA it behaves like an uncompetitive type of inhibitor whereas for core histones, as a competitive inhibitor. These differences in the inhibition pat-

TABLE I
Inhibition kinetic parameters

Substrate	K_m	V_{max}	k_{cat}/s	Substrate	K_m	V_{max}	k_{cat}/s
	μM				μM		
p300							
Histones	0.03	6250	0.69	Acetyl-CoA	0.25	7468	0.82
5 μM garcinol	0.095	6250	0.69	5 μM garcinol	0.42	6501	0.72
7 μM garcinol	0.151	6250	0.69	7 μM garcinol	0.53	5288	0.58
PCAF							
Histones	0.028	5175	0.57	Acetyl-CoA	0.177	4889	0.53
5 μM garcinol	0.099	5175	0.57	5 μM garcinol	0.227	3487	0.38
7 μM garcinol	0.169	5175	0.57	7 μM garcinol	0.282	2751	0.30

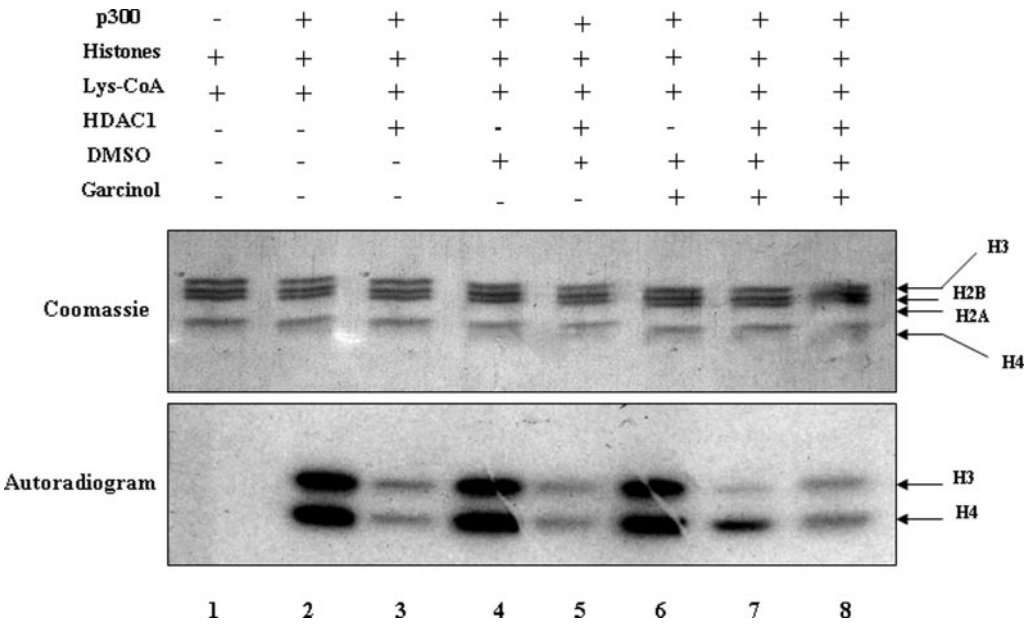

FIG. 4. **Garcinol does not affect the histone deacetylase activity of histone deacetylase 1.** 2.4 μg of ^{3}H-labeled highly purified HeLa core histones (by p300) were subjected to deacetylation with 60 ng of recombinant HDAC 1 in the presence (10 and 20 μM) or absence of garcinol. *Lane 1*, unlabelled histones; *lane 2*, acetylated histones; *lane 3*, acetylated histones treated with HDAC1; *lane 4*, acetylated histones treated with Me_2SO (*DMSO*); *lane 5*, deacetylation of histones in the presence of Me_2SO (*DMSO*); *lane 6*, acetylated histones with garcinol (10 μM); *lanes 7* and *8*, deacetylation of acetylated histones by HDAC1 in the presence of 10 μM and 20 μM garcinol, respectively.

tern indicate the mechanistic uniqueness of garcinol.

In order to ensure enzyme specificity as well as substrate specificity we went on to check the effect of garcinol on the HDAC1 enzyme. The HDAC assay protocol was followed as described previously (31). Deacetylation of core histones in the presence or absence of the compound, garcinol (10 or 20 μM) shows no difference whatsoever (Fig. 4, *lanes 7* and *8 versus lane 3*). Addition of the solvent of garcinol, Me_2SO, has no effect on the deacetylation of core histones by the recombinant HDAC1 (Fig. 4, *lane 5*). Therefore we can presume that garcinol is specific to HAT activity. In order to verify this HAT specificity we used the HAT-dependent *in vitro* chromatin transcription assay system as described previously (12). The chromatin template was assembled on pG5-ML-array (12) by employing the NAP1 assembly system. The assembled chromatin was characterized by DNA supercoiling and partial micrococcal (MNase) digestion assay (Fig. 5, *B* and *C*). As depicted in the figure, a substantial amount of relaxed DNA was found to be supercoiled upon deposition of nucleosome (Fig. 5*B*, *lane 2 versus lane 3*). Because the supercoiling assay does not assure the proper spacing of the histone octamer, partial micrococcal digestion was performed wherein we found 4 to 5 well resolved regularly spaced nucleosomes (Fig. 5*C*). The results of these assays suggest that the assembled chromatin is appropriate for *in vitro* transcription experiments. The transcription assay followed the protocol depicted in Fig. 5*A*. To establish the HAT-specific nature of garcinol, we tested its effect on transcription from DNA, which is not HAT-dependent (Fig. 5*D*). The chimeric transcriptional activator, Gal4-VP16 activates transcription around 10-fold compared with basal transcription without any activator (Fig. 5*D*, *lane 2 versus 1*). Addition of solvent (Me_2SO) or 20 μM and 50 μM garcinol shows no effect on the activator-dependent transcription (Fig. 5*D*, *lanes 3–5*). The activator-independent transcription from the ML200 promoter was used as a loading control. As reported previously, transcription from the chromatin template shows complete dependence on acetylation (absolute requirement of acetyl-CoA), as depicted in Fig. 5*E* (*lane 3 versus 4*). Addition of Me_2SO, marginally represses the transcription (Fig. 5*E*, *lane 4 versus 5*). Interestingly, increasing concentrations of garcinol (especially 50 μM) dramatically represses HAT-dependent chromatin transcription (Fig. 5*E*, *lane 5 versus 7*). These data show that garcinol specifically inhibits HAT activity-dependent chromatin transcription but not transcription from the DNA template.

We have shown that garcinol is a potent inhibitor of HATs both *in vitro* and *in vivo*. Furthermore, it also inhibits the HAT-dependent transcription from chromatin template. In order to further understand its effect *in vivo*, we treated the HeLa cells with increasing concentrations of garcinol and performed the apoptosis assay. The effect of garcinol on chromatin fragmentation was investigated for this purpose. HeLa cells treated with hydrogen peroxide to induce the apoptosis were taken as

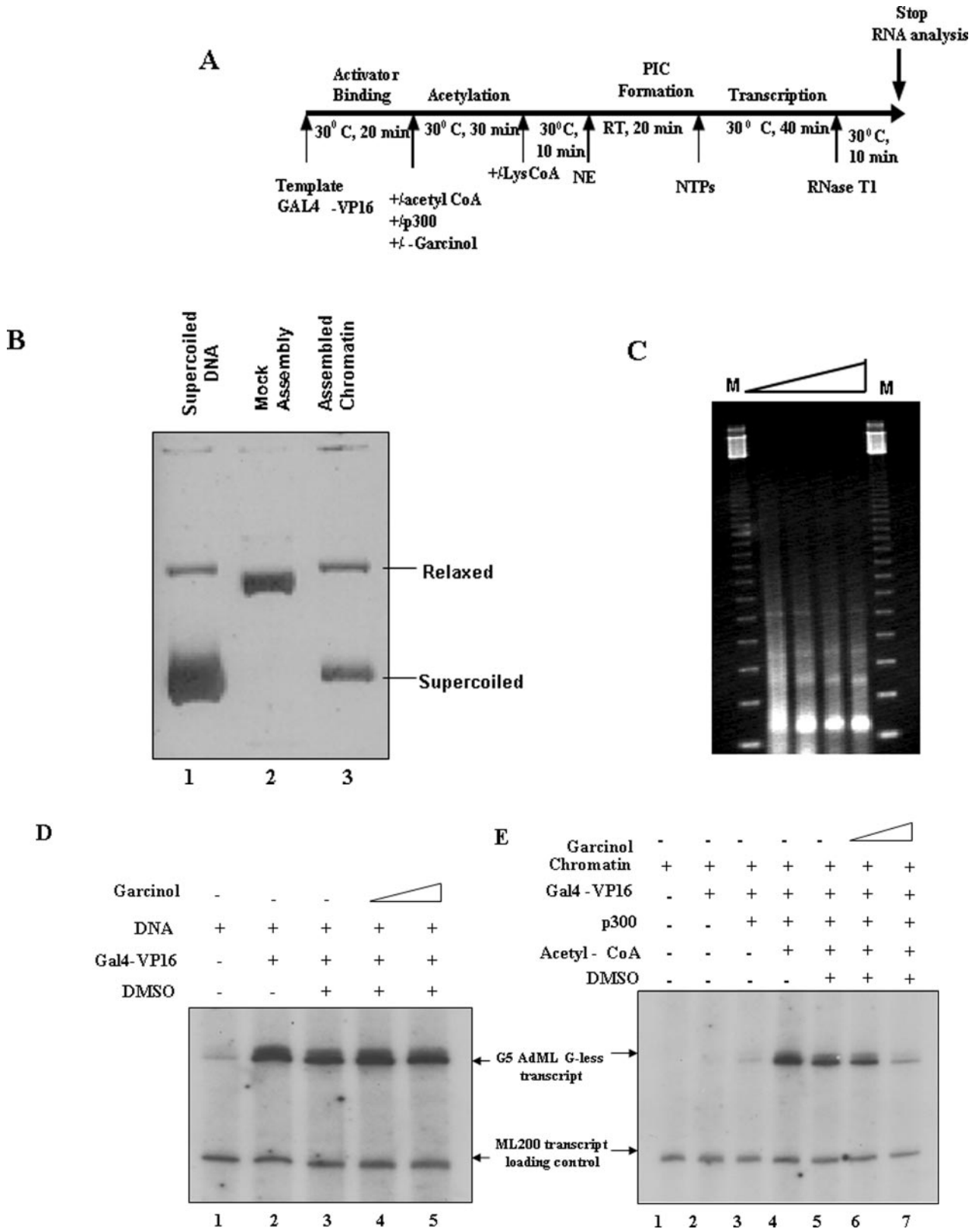

FIG. 5. **Garcinol inhibits p300 HAT activity-dependent transcriptional activation from the chromatin template.** *A*, schematic representation of the *in vitro* transcription protocol. *B*, DNA supercoiling assay for assembled chromatin. *Lane 1*, supercoiled DNA used for assembly; *lane 2*, relaxed DNA (after dTopoI treatment of the DNA of *lane 1*); *lane 3*, chromatinized DNA isolated by deproteinization. *C*, MNase digestion pattern of assembled chromatin. The chromatin was treated with increasing concentrations of MNase at room temperature. After deproteinization, the resulting DNA was resolved on a 1.5% agarose gel and stained with ethidium bromide. *In vitro* transcription from naked DNA (*D*) and chromatin template (*E*). 30 ng of DNA and freshly assembled chromatin template (equivalent to 30 ng of DNA) were subjected to the protocol in *A* with or without garcinol, 50 ng of Gal4-VP16, 25 ng of baculovirus-expressed highly purified His_6-tagged p300 (full-length) and 1.5 μM acetyl-CoA. The *in vitro* transcription reaction mixtures were analyzed on 5% urea-acrylamide gel and further processed by autoradiography. *D*, *lane 1*, without activator (basal transcription); *lane 2*, with activator (Gal4-VP16); *lane 3*, with activator and Me_2SO; *lanes 4 and 5*, with activator and 20 and 50 μM garcinol. *E*, *lane 1*, without activator; *lane 2*, with activator; *lane 3*, with activator and p300, *lane 4*, with activator, p300 and acetyl-CoA, *lane 5*, reaction of *lane 4* in the presence of Me_2SO, *lanes 6* and *7*, reaction of *lane 4* in the presence of 20 and 50 μM garcinol.

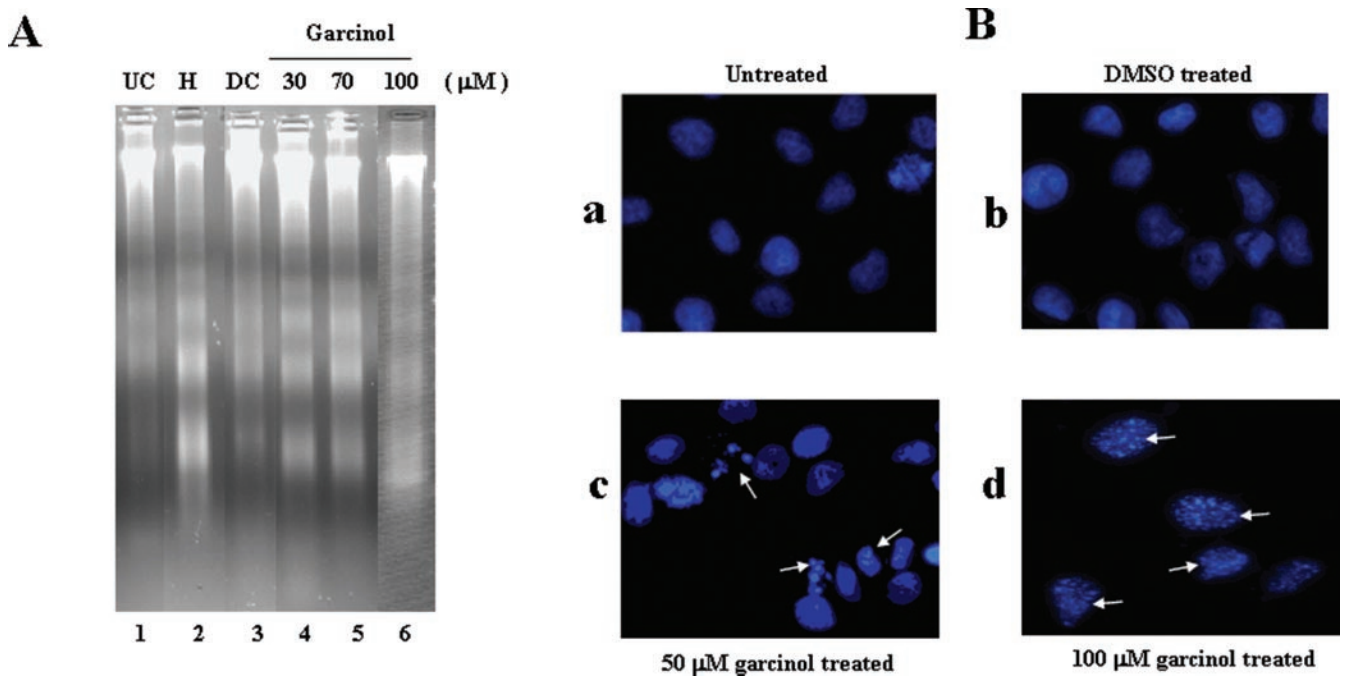

FIG. 6. **Garcinol induces apoptosis in HeLa cells.** HeLa cells grown in monolayer were treated with garcinol and subjected to apoptosis assay. *A*, agarose gel electrophoresis of the DNA extracted from the compound-treated cells. Fragmentation of nucleosomal DNA was visualized by ethidium bromide staining. *Lane 1*, untreated cells; *lane 2*, hydrogen peroxide-treated; *lane 3*, Me_2SO-treated; and *lanes 4–6*, cells treated with 30, 70, and 100 μM garcinol respectively. *B*, Hoechst staining of HeLa cells treated with Me_2SO (*DMSO*) (*panel b*) and 50 and 100 μM garcinol (*panels c* and *d*). *Panel a* shows untreated control. *Arrows* indicate apoptotic nuclear fragmentation.

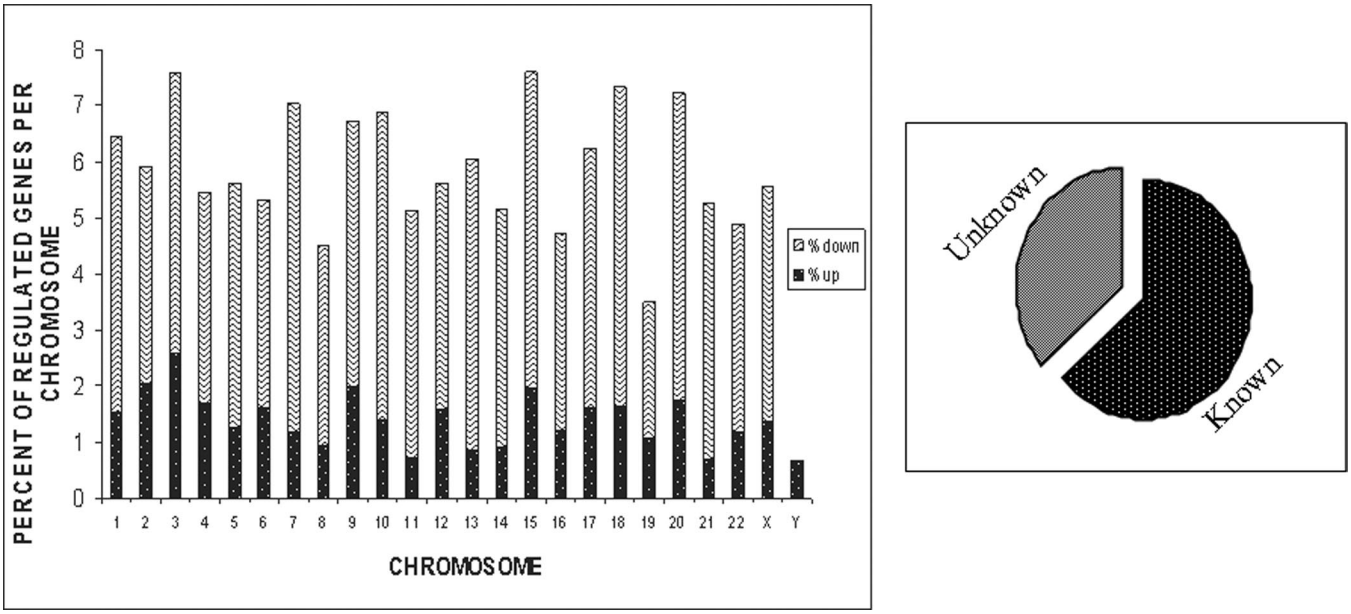

FIG. 7. **The percent of differentially expressed genes per chromosome are represented as a bar graph.** The *pie chart* represents the known and unknown fraction of differentially expressed genes.

a positive control to test garcinol-mediated apoptosis. Fragmented chromatin was analyzed on a 1.8% agarose gel (Fig. 6*A*). The cells treated with buffer or solvent (Me_2SO) did not show any obvious differences (Fig. 6*A*, *lanes 1 versus 3*), but treatment with hydrogen peroxide yielded huge amounts of faster moving species of DNA fragments (Fig. 6*A*, *lane 2*). Similar to hydrogen peroxide treatment, increasing concentrations of garcinol (30, 70, and 100 μM) also induce apoptosis and generate smaller DNA fragments (Fig. 6*A*, compare *lane 2* with *4* and *6*). To visualize the chromatin fragmentation *in situ*, compound-treated nuclei were stained with Hoechst (which stains the DNA). In agreement with the DNA fragmentation data Hoechst staining of the nuclei also shows that treatment with 50 and 100 μM garcinol induces the fragmentation of nuclei, as indicated by *arrows* (Fig. 6*B*, *panels c* and *d*). Taken together these data show that the histone acetyltransferase inhibitor garcinol stimulates the apoptosis in HeLa cells.

The histone acetyltransferase specificity, induction of apoptosis, and more significantly the ability of garcinol to inhibit the histone acetylation *in vivo* prompted us to investigate its effect on global gene regulation. HeLa cells were treated with 100 μM garcinol for 24 h and subjected to microarray analysis to investigate its effect on global gene regulation. Genome wide analysis of gene expression using microarrays indicates

TABLE II
Genes differentially expressed with treatment of the HAT inhibitor, garcinol

Category	ACCID[a]	Genes down-regulated
Apoptosis	R70836	BCL2-like 2
	W25164	BCL-6 interacting corepressor
	R12025	Bifunctional apoptosis regulator
	T78664	Death-associated protein kinase 1
	R26621	Fas apoptotic inhibitory molecule 2
	R32216	p53-induced protein PIGPC1
Cell cycle	N41329	ATP-binding protein associated with cell differentiation
	AA034317	Candidate tumor suppressor protein
	H10087	Cyclin A1
	BG397188	Cyclin-dependent kinase 5
	W94879	HIR histone cell cycle regulation defective homolog A (*S. cerevisiae*)
	R77519	Myeloid cell nuclear differentiation antigen
	H15206	NIMA (never in mitosis gene a)-related kinase 3
	R13675	p21(CDKN1A)-activated kinase 6
	H10435	BRCA1-associated protein
Oncogene	BM549678	Cervical cancer 1 protooncogene
	BI255100	Cervical cancer 1 protooncogene
	W03558	Hepatocellularcarcinoma-associated antigen HCA557a
	H49173	Melanoma-associated gene
	AA040629	Myeloid/lymphoid or mixed-lineage leukemia (trithorax homolog, *Drosophila*); translocated to, 6
	H10435	Ovarian carcinoma immunoreactive antigen
	H10546	Pim-2 oncogene
	AA133961	Pituitary tumor-transforming 1-interacting protein
	R55296	Promyelocytic leukemia
	H23370	RAB22A, member RAS oncogene family
	H02076	T-cell leukemia/lymphoma 1A
	R37897	Tumor protein p63
	BQ019936	Tumor protein, translationally-controlled 1
	W91952	vav 3 oncogene
	BF434098	v-maf musculoaponeurotic fibrosarcoma oncogene homolog (avian)
	H29655	v-rel reticuloendotheliosis viral oncogene homolog B, nuclear factor of kappa light polypeptide gene enhancer in B-cells 3 (avian)
	AA005328	v-ski sarcoma viral oncogene homolog (avian)
Transcription factors	R66029	Bromodomain adjacent to zinc finger domain, 1A
	BM548888	Bromodomain and PHD finger containing, 1
	R18948	Cofactor required for Sp1 transcriptional activation, subunit 2, 150kDa
	R14275	Cofactor required for Sp1 transcriptional activation, subunit 2, 150kDa
	H84735	DNA-directed RNA polymerase II polypeptide J-related gene
	AA161069	E1B-55kDa-associated protein 5
	T96195	E74-like factor 4 (ets domain transcription factor)
	R06038	General transcription factor II, I
	R76588	General transcription factor IIIA
	AA010526	Glucocorticoid receptor DNA-binding factor 1
	BF793857	High-mobility group nucleosome-binding domain 1
	H83982	High-mobility group nucleosome-binding domain 1
	T80557	High-mobility group protein 2-like 1
	R59260	MADS box transcription enhancer factor 2, polypeptide C (myocyte enhancer factor 2C)
	BQ003252	MADS box transcription enhancer factor 2, polypeptide C (myocyte enhancer factor 2C)
	W69683	Nuclear factor (erythroid-derived 2)-like 1
	T77709	Nuclear factor of kappa light polypeptide gene enhancer in B-cells 1 (p105)
	N43877	Nuclear receptor subfamily 4, group A, member 3
	W35230	Putative DNA/chromatin-binding motif
	BE880112	Sp2 transcription factor
	H82615	Special AT-rich sequence-binding protein 1 (binds to nuclear matrix/scaffold-associating DNA's)
	W35313	Sterile α-motif and leucine zipper containing kinase AZK
	BM904501	TAF12 RNA polymerase II, TATA box-binding protein (TBP)-associated factor, 20 kDa
	BE871226	TAF6 RNA polymerase II, TATA box-binding protein (TBP)-associated factor, 80 kDa
	R11718	Transcription factor 4
	AA029516	Transcription factor 7-like 2 (T-cell specific, HMG-box)
	BI907810	Transcription factor B2, mitochondrial
	R86677	Zinc finger protein 3 (A8–51)
	T99177	Zinc finger protein 317
	R12731	Zinc finger protein 335
	AA043477	Zinc finger protein 36, C3H type, homolog (mouse)

Category	ACCID	Genes up-regulated
Apoptosis	H45000	Caspase 4, apoptosis-related cysteine protease
	R13349	CED-6 protein
Cell cycle	AA055894	Anaphase-promoting complex 1 (meiotic checkpoint regulator)
	W85770	BUB1 budding uninhibited by benzimidazoles 1 homolog β (yeast)
	W40330	G_1 to S phase transition 1
	R97935	Cell division cycle 34
Oncogene	H85307	v-K_i-ras2 Kirsten rat sarcoma 2 viral oncogene homolog
	R67109	RAB9A, member RAS oncogene family

TABLE II—*continued*

Category	ACCID[a]	Genes down-regulated
Transcription factor	T74980	Basic leucine zipper nuclear factor 1 (JEM-1)
	H66228	Core-binding factor, runt domain, α-subunit 2; translocated to, 3
	R39405	Dishevelled, dsh homolog 2 (*Drosophila*)
	AA101861	Heat shock transcription factor 4
	R55134	HMG-box transcription factor TCF-3
	AA043380	Homeobox D10
	R09787	MBD2 (methyl-CpG-binding protein)-interacting zinc finger protein
	AA045325	msh homeobox homolog 1 (*Drosophila*)
	R78177	Paired-like homeodomain transcription factor 2
	N92222	Putative homeodomain transcription factor 1
	R71263	TAF4 RNA polymerase II, TATA box-binding protein (TBP)-associated factor, 135 kDa
	R67748	Transcriptional adaptor 2 (ADA2 homolog, yeast)-like
	R39430	Transcriptional intermediary factor 1
	H14414	Zinc finger protein 195
	T80906	Zinc finger protein 28 homolog (mouse)
	R23489	Zinc finger protein 354A

[a] ACCID, GenBank™ accession identification number.

that treatment of HeLa cells with garcinol causes the down-regulation of a larger number of genes (1631 genes) compared with up-regulation (630 genes). As shown in the *inset* in Fig. 7, out of 2261 differentially regulated genes, 1445 genes have been annotated, and 816 genes are either ESTs or are unknown genes. We sorted out the annotated genes based on the chromosomal localization and represented this as a bar graph with differentially regulated genes shown per chromosome (Fig. 7). It is evident that on most chromosomes the number of down-regulated genes is higher except on chromosome Y, where there were no down-regulated genes. When normalized for the total number of genes known per chromosome, it turns out that ~6–8% of the known genes in almost all the chromosomes were found to be differentially regulated on treatment with garcinol.

We classified the differentially regulated genes in various functional categories based on the available annotation in the public data bases and that supplied by the slide manufacturer. Some of the interesting categories and the genes that were either up- or down-regulated are listed in Table II. Among the up-regulated genes are those for caspase 4 and CED6, which are pro-apoptotic whereas anti-apoptotic genes like the BCL2 family members and the Fas inhibitory molecule are among the down-regulated genes. The ubiquitin-conjugating enzyme and the E3 ubiquitin ligase are up-regulated, which supports the observed death of treated cells by apoptosis. It was also found that the genes for the p53-induced protein PIGPC1 and p21 (CDKN1A)-activated kinase 6, which are down-regulated probably because they are targets of p53 and p21, respectively, which in turn are regulated by the p300/PCAF histone acetyltransferases. Proto-oncogenes form a class of genes of which more are down-regulated than up-regulated by this treatment, emphasizing the role of garcinol as a molecule with anti-cancer activity. Large numbers of differentially regulated genes involved in metabolism and those categorized as transcription factors or signal transducers have not been included in the table because of space constraints. The exact significance of the result is yet to be determined. A large number of unannotated genes that may have a significant role in cellular functioning are found to be differentially regulated.

As suggested in a recent review (1), the development of small molecular weight HAT inhibitors and activators as therapeutic targets is the next step, following the HDAC inhibitors; some of which are being tested in clinical trials. Here we show for the first time that garcinol, a polyisoprenylated benzophenone from *G. indica* fruit rind is a small molecule, HAT inhibitor that can be taken in by cells. There are very few HAT inhibitors known to date. The first reported HAT inhibitors were bisubstrate (29) types of inhibitors of p300 and PCAF, which contain CoA moieties. One of these compounds, Lys-CoA has proven useful for blocking the HAT activity of p300 specifically. Though it has been employed for *in vitro* transcription studies (12) and in cells via microinjection or with the use of cell-permeabilizing agents (41), Lys-CoA has generally been ineffective with simple addition to cell culture media. The cells were also found to be not permeable to a PCAF-specific inhibitor of the same group, H3-CoA-20, which contains CoA-conjugated to a 20-amino acid residue peptide from the N terminus of histone H3. Recently we have isolated the first naturally occurring HAT inhibitor, anacardic acid (AA), which inhibits the HAT activity of both p300 and PCAF very effectively (31). By using AA as a synthon we have synthesized an amide derivative of anacardic acid CTPB, which is the only known small molecule activator of any histone acetyltransferase (p300). Significantly, CTPB is exclusively specific for p300 HAT activity. However cells are not permeable or poorly permeable to both anacardic acid and CTPB.[2]

We have demonstrated that garcinol not only inhibits the histone acetylation by p300 and PCAF *in vitro* (Fig. 2, *A* and *B*), it also represses the acetylation *in vivo* in HeLa cells (Fig. 2*C*). In correlation with this observation and earlier report (42), garcinol induces apoptosis of HeLa cells in a concentration-dependent manner. Garcinol is known to possess antioxidant and anticancer chemopreventive activity (Refs. 42 and 43 and references therein). Recently it has been shown that garcinol induces apoptosis in human leukemia cell lines (44). The present finding of garcinol as an inhibitor of histone acetyltransferases may help to further understand the mechanism of garcinol-induced apoptosis.

Presumably, hypoacetylation of histone is a prerequisite of apoptosis. Though the relationship between acetylation of histones and activation of gene expression is not as direct as it was believed to be, overall acetylation is a diagnostic feature of active genes. Thus inhibition of acetylation *in vivo* would repress the majority of the genes. Our microarray analysis of garcinol-treated HeLa cell gene expression indeed showed that more than 72% of genes (tested) were down-regulated. (Fig. 7 and Table II). The microarray data further revealed that several proto-oncogenes are down-regulated in the presence of garcinol, suggesting that garcinol may function as an anticancer compound. However, a systematic investigation using normal (untransformed) and different cancerous cell lines are essential to elucidate the specific role of garcinol for cancer prevention. Because alteration of histone acetylation also has a causal relation with the manifestation of other diseases,

[2] R. A. Varier and T. K. Kundu, unpublished data.

namely asthma (45) and AIDS, garcinol or its derivatives may serve as lead compounds for designing therapeutic targets for other diseases in addition to cancer.

Acknowledgments—We thank Drs. James Kadonaga and Yoshihiro Nakatani for providing invaluable reagents.

REFERENCES

1. Roth, S. Y., Denu, J. M., and Allis, C. D. (2001) *Annu. Rev. Biochem.* **70,** 81–120
2. Berger, S. L. (2002) *Curr. Opin. Genet. Dev.* **12,** 142–148
3. Sterner, D. E., and Berger, S. L. (2000) *Microbiol. Mol. Biol. Rev.* **64,** 435–459
4. Marks, P. A., Rifkind, R. A., Richon, V. M., Breslow, R., Miller, T., and Kelly, W. K. (2001) *Nat. Rev. Cancer.* **1,** 194–202
5. Shikama, N., Lyon, J., and La Thangue, N. B. (1997) *Trends Cell Biol.* **7,** 230–236
6. Wolffe, A. P. (2001) *Oncogene* **20,** 2988–2990
7. Rouaux, C., Jokic, N., Mbebi Boutiller, S., Leoffler, J. P., and Boutiller, A. L. (2003) *EMBO J.* **22,** 6537–6549
8. Puri, P. L., Sartorelli, V., Yang, X. J., Hamamori, Y., Ogryzko, V., Howard, B. H., Kedes, L., Wang, J. Y., Graessmann, A., Nakatani, Y., and Levrero, M. (1997) *Mol. Cell.* **1,** 35–45
9. Spacer, T. E., Jenster, G., Burcin, M. M., Allis, C. D., Zhou, J., Mizzen, C. A., McKenna, N. J., Onate, S. A., Tsai, M. J., and O'Malley, B. W. (1997) *Nature* **389,** 194–198
10. Hung, H. L., Lau, J., Kim, A. Y., Weiss, M. J., and Blobel, G. A. (1999) *Mol. Cell. Biol.* **19,** 3496–3505
11. Chen, H., Lin, R. J., Xie, W., Wilpitz, D., and Evans, R. M. (1999) *Cell* **98,** 675–686
12. Kundu, T. K., Palhan, V., Wang, Z., An, W., Cole, P. A., and Roeder, R. G. (2000) *Mol. Cell* **6,** 551–561
13. An, W., Palhan, V. B., Karymov, M. A., Leuba, S. H., and Roeder, R. G. (2002) *Mol. Cell* **9,** 811–821
14. Yang, X. L., Ogryzko, V. V., Nishikawa, J., Howard, B. H., and Nakatani, Y. A. (1996) *Nature* **382,** 319–324
15. Schiltz, R. L., and Nakatani, Y. (2000) *Biochim. Biophys. Acta, Rev. Cancer* **1470,** M37–M53
16. Yamauchi, T., Yamauchi, J., Kuwata, T., Tamura, T., Yamashita, T., Bae, N., Westphal, H., Ozata, K., and Nakatani, Y. (2000) *Proc. Natl. Acad. Sci. U. S. A.* **97,** 11303–11306
17. Ogryzko, V. V., Kotani, T., Zhang, X., Schiltz, R. L., Howard, T., Yang, X. J., Howard, B. H., Qin, J., and Nakatani, Y. (1998) *Cell* **94,** 35–44
18. Kumar, P. B. R., Swaminathan, V., Banerjee, S., and Kundu, T. K. (2001) *J. Biol. Chem.* **276,** 16804–16806
19. Bonaldi, T., Talamo F., Scaffidi, P., Ferrera, D., Porta, A., Bachi, A., Rubartelli, A., Agresti, A., and Bianchi, E. (2003) *EMBO J.* **22,** 5551–5560
20. Kaehlcke, K., Dorr, A., Hetzer-Egger, C., Kiermer, V., Henklein, P., Schnoelzer, M., Loret, E., Cole, P. A., Verdin, E., and Ott, M. (2003) *Mol. Cell* **12,** 167–176
21. Bres, V., Tagami, H., Peloponese, J. M., Loret, E., Jeang, K. T., Nakatani, Y., Emiliani, S., Benkirane, M., and Kiernan, R. E. (2002) *EMBO J.* **21,** 6811–6819
22. Borrow, J., Stanton, V. P., Jr., Andresen, J. M., Becher, R., Behm, F. G., Chaganti, R. S., Civin, C. I., Disteche, C., Dube, I., Frischauf, A. M., Horsman, D., Mitelman, F., Volinia, S., Watmore, A. E., and Housman, D. E. (1996) *Nat. Genet.* **14,** 33–41
23. Murata, T., Kurokawa, R., Krones, A., Tatsumi, K., Ishii, M., Taki, T., Masuno, M., Ohashi, H., Yanagisawa, M., Rosenfeld, M. G., Glass, C. K., and Hayashi, Y. (2001) *Hum. Mol. Genet.* **10,** 1071–1076
24. Kalkhoven, E., Roelfsema, J. H., Teunissen, H., Den Boer, A., Ariyurek, Y., Zantema, A., Breuning, M. H., Hennekam, R. C., and Peters, D. J. (2003) *Hum. Mol. Genet.* **12,** 441–450
25. Lusic, M., Marcello, A., Cereseto, A., and Giacca, M. (2003) *EMBO J.* **22,** 6550–6561
26. Quivy, V., Adam, E., Collette, Y., Demonte, D., Chariot, A., Vanhulle, C., Berkhout, B., Castellano, R., De Launoit, Y., Burny, A., Piette, J., Bours, V., and Van Lint, C. (2002) *J. Virol.* **76,** 11091–11103
27. Richon, V. M., Zhou, X., Rifkind, R. A., and Marks, P. A. (2001) *Blood Cells Mol. Dis.* **27,** 260–264
28. Cullis, P. M., Wolfenden, R., Cousens, L. S., and Alberts, B. M. (1982) *J. Biol. Chem.* **257,** 12165–12169
29. Lau, O. D., Kundu, T. K., Soccio, R. E., Ait-Si-Ali, S., Khalil, E. M., Vassilev, A., Wolfee, A. P., Nakatani, Y., Roeder, R. G., and Cole, P. A. (2000) *Mol. Cell.* **5,** 589–595
30. Cebrat, M., Kim, C. M., Thompson, P. R., Daugherty, M., and Cole, P. A. (2003) *Bioorg. Med. Chem.* **11,** 3307–3313
31. Balasubramanyam, K., Swaminathan, V., Ranganathan, A., and Kundu, T. K. (2003). *J. Biol. Chem.* **278,** 19134–19140
32. Kundu, T. K., Wang, Z., and Roeder, R. G. (1999) *Mol. Cell. Biol.* **19,** 1605–1615
33. Shaiu, W., and Hsieh, T. (1998) *Mol. Cell. Biol.* **18,** 4358–4367
34. Chambers, A. E., Banerjee, S., Chaplin, T., Dunne, J., Debernardi, S., Joel, S. P., and Young, B. D. (2003) *Eur. J. Cancer.* **39,** 1165–1175
35. Ryan, C. A., and Annunziato, A. T. (2001) in *Current Protocols in Molecular Biology* (Canada, V., ed) pp. 2.3–2.10, John Wiley and Sons Inc., New York
36. Bonner, W. M., West, M. H., and Stedman, J. D. (1980) *Eur. J. Biochem.* **109,** 17–23
37. Pillai, B., Brahmachari, S. K., and Sadhale, P. P. (2001) *Curr. Sci.* **81,** 574–578
38. Wolffe, A. (1998) *Chromatin Structure and Function*, pp. 97–105, Academic Press, New York
39. Tanner, K. G., Langer, M. R., and Denu, J. M. (2000) *Biochemistry.* **39,** 11961–11969
40. Thompson, P. R., Kurooka, H., Nakatani, Y., and Cole, P. A. (2001) *J. Biol. Chem.* **276,** 33721–33729
41. Polesskaya, A., Naguibneva, I., Fritsch, L., Duquet, A., Ait-Si-Ali, S., Robin, P., Vervisch, A., Pritchard, L. L., Cole, P. A., and Harel-Bellan, A. (2001) *EMBO J.* **20,** 6816–6825
42. Pan, M. H., Chan, W. L., Lin-Shiau, S. Y., and Lin, J. K. (2001) *J. Agric. Food Chem.* **49,** 1464–1474
43. Ito, C., Itoigawa, M., Miyamoto, Y., Onoda, S., Rao, K.S., Mukainaka, T., Tokuda, H., Nishino, H., and Farukawa, H. (2003) *J. Nat. Prod.* **66,** 206–209
44. Matsumoto, K., Akao, Y., Kobayashi, E., Ito, T., Ohguchi, K., Tanaka, T., Linuma, M., and Nozawa, Y. (2003) *Biol. Pharm. Bull.* **26,** 569.–571
45. Kagoshima, M., Ito, K., Cosio, B., and Adcock, I. M. (2003) *Biochem. Soc. Trans.* **31,** 61–65
46. Yamaguchi, F., Saito, M., Ariga, T., Yoshimura, Y., and Nakazawa, H. (2000) *J. Agric. Food Chem.* **48,** 2320–2325